Supplement of Hydrol. Earth Syst. Sci., 30, 2879–2911, 2026
https://doi.org/10.5194/hess-30-2879-2026-supplement

Hydrology and Earth System Sciences
Open Access

Supplement of

From soil to stream: modeling the catchment-scale hydrological effects of increased soil organic carbon

Malve Heinz et al.

Correspondence to: Malve Heinz (malve.heinz@unibe.ch)

Supplementary Material

S1 Comparison of model performance with studies in the same catchment

Previous studies covering the Broye catchment show varying performance: Zarrineh et al. (2018) calibrated SWAT over 1986–2014, achieving an NSE of 0.60 (calibration) and 0.66 (validation) for daily discharge. Their calibration prioritized low flows, resulting in underestimation of peak flows. Notably, they used precipitation from three local weather stations, which may explain the absence of precipitation bias in their results. Muelchi et al. (2021) applied PREVAH (Viviroli et al., 2009) using projected climate data. For the reference period, model skill was moderate (KGE = 0.69, NSE = 0.51) with a positive precipitation bias of +14.5%. Brunner et al. (2019), also using PREVAH but with (observed) RhiresD precipitation data, reported a KGE of 0.74 and NSE of 0.73 for 1981–2016. However, if we only test the 2010–2016 period (same length as our study period), performance improved (KGE = 0.96, NSE = 0.68). Still, a substantial +22% precipitation bias was noted. Michel et al. (2022) employed Alpine3D (Lehning et al., 2006) with observed station precipitation data, achieving a KGE = 0.77 over 2003–2018. Their flow duration curves indicate a tendency to overestimate high flows and underestimate low flows. These comparisons underline the importance of input data quality. Studies using RhiresD precipitation tend to show positive precipitation biases, while those using station data do not. Although our method of correcting the bias in RhiresD is very simplified, it reduced the positive precipitation bias that was also found in the study of Brunner et al. (2019).

S2 SOC increase results for more states and fluxes

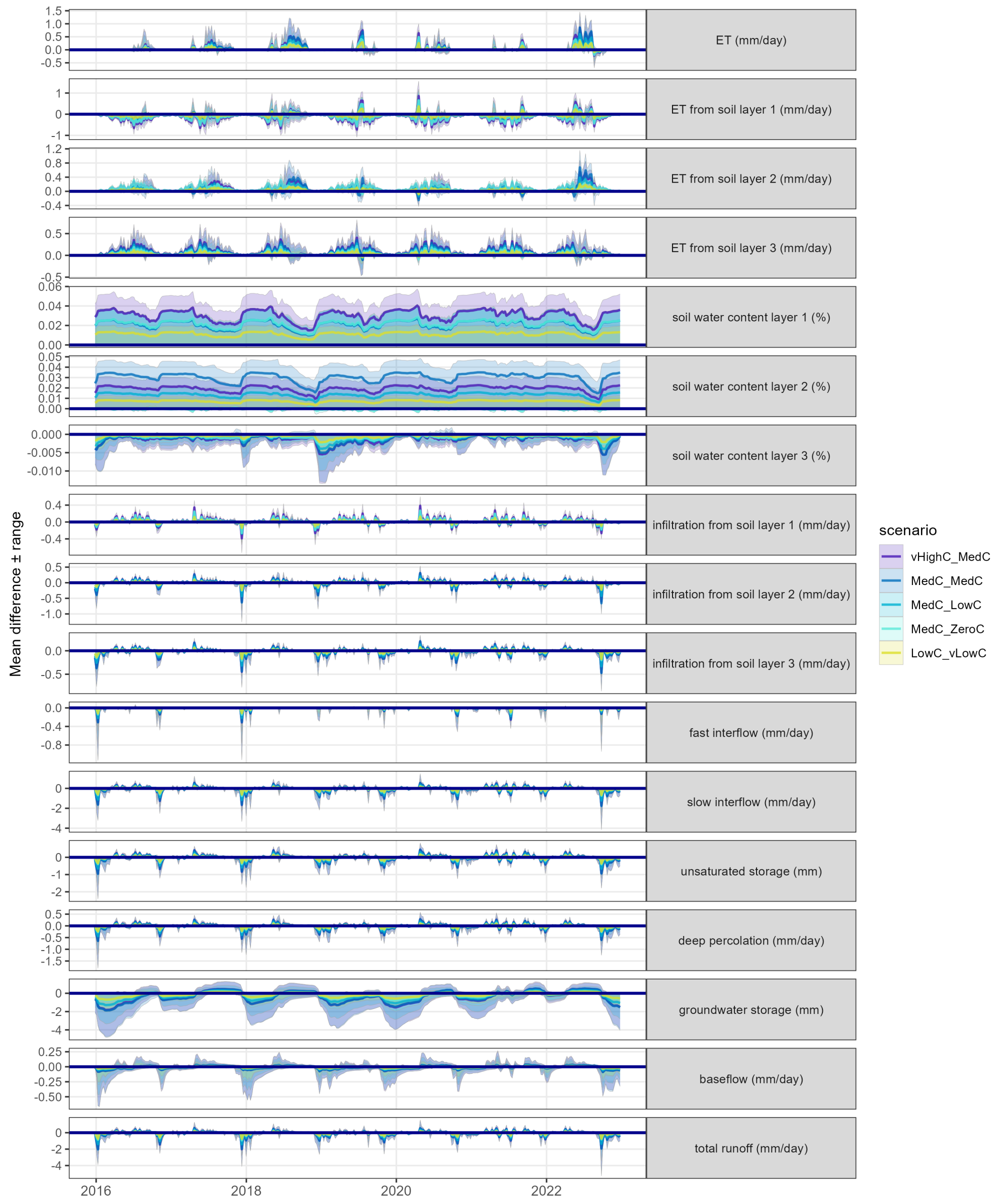

Figure S1. Weekly aggregated differences in states and fluxes for SOC scenarios vs. base scenario

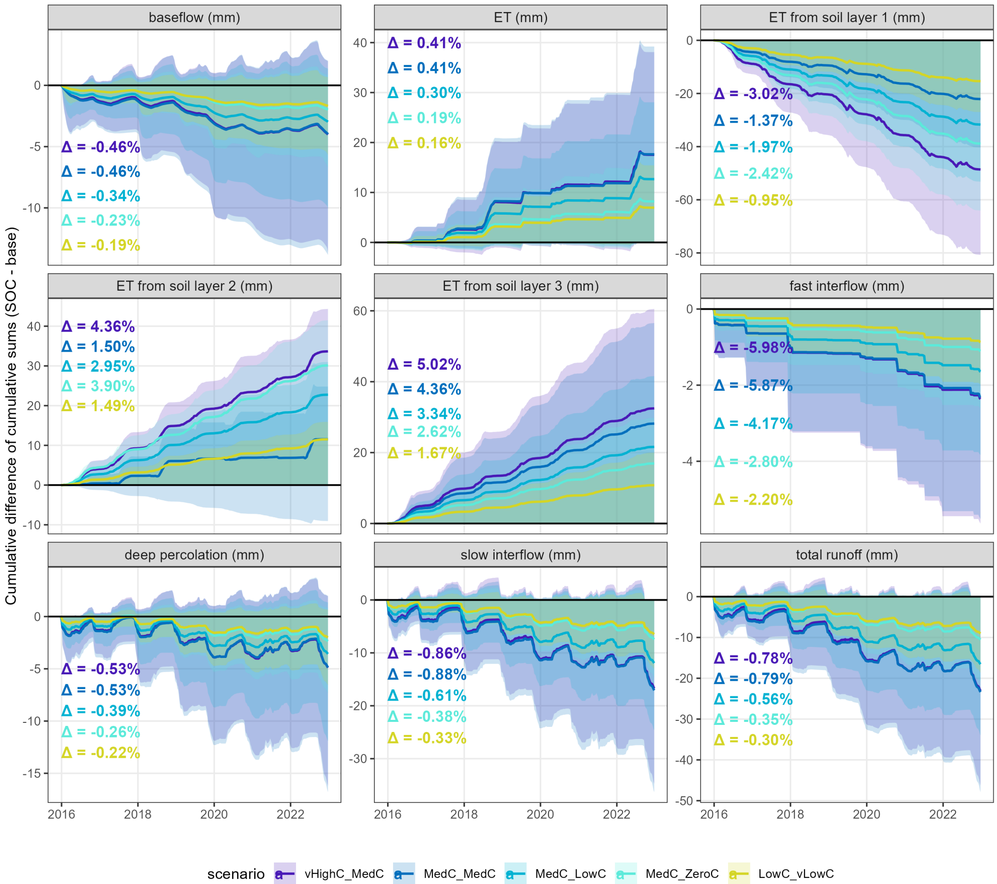

Figure S2. Cumulative difference of cumulative sums for all fluxes for SOC scenarios vs. base scenario

S3 Evaluation of alternative precipitation products as inputs to mHM

As reported in Section 3.2, we were not expecting such distinct differences in annual discharge (mm) between the different subcatchments (Appendix A1). The Petit Glâne and the Arbogne must either much less precipitation, or much more water is extracted from the rivers, we assume it is a combination of both factors, since there are no information on the actual water withdrawal amounts available. We assume, that the relatively high annual precipitation in relation to the low discharge could also be the results of an interpolation artifact. We compared the skill of different precipitation products to assess if one would reduce the bias. The compared products are: timeseries of different MeteoSwiss stations (MeteoSwiss, 2025b), the gridded precipitation product RhiresD (MeteoSwiss, 2021), the hourly, stochastic and radar based precipitation product CPC (MeteoSwiss, 2025a) and the probabilistic precipitation ensemble dataset RhydCHprob (MeteoSwiss and Climatology, 2019). Due to the different nature of each product, we try to compare those that cover the same or a similar area.

Table S1. Overview of available data sources by area.

nr	area	Available data by:
1	Payerne (meteostation location)	MeteoSwiss, RhiresD, CPC, RhydCHprob
2	Chables (meteostation location)	MeteoSwiss, RhiresD, CPC, RhydCHprob
3	Avenches (meteostation location)	MeteoSwiss, RhiresD, CPC, RhydCHprob
5	Petit Glane (subcatchment)	RhiresD, CPC, RhydCHprob
6	Arbogne (subcatchment)	RhiresD, CPC, RhydCHprob
7	+/- 0.05° box around Payerne	RhiresD, CPC, RhydCHprob
8	Agrometeo (meteostation)	Agrometeo

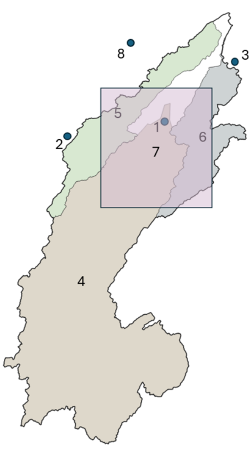

Figure S3. Location of areas reference in Table S1

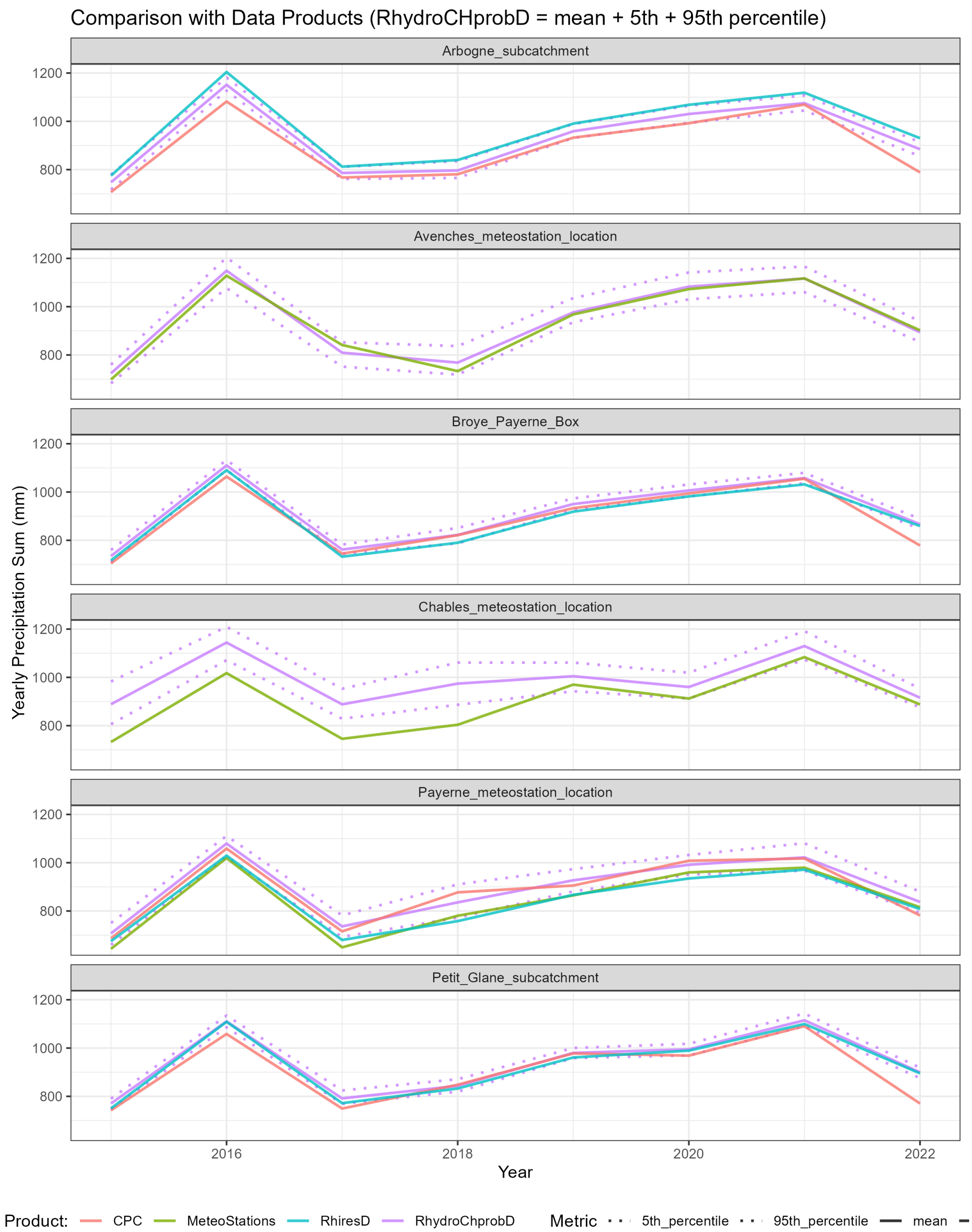

Figure S4. Comparison of annual precipitation sum of different precipitation data products for different locations

Since we could not identify a clear advantage of any of the alternative gridded precipitation products, we decided to keep using the RhiresD dataset with a very simply correction method. Since we saw that nearby meteostations actually showed slightly less precipitation then the RhiresD for subcatchments Petit Glâne and Arbogne, we replaced the gridded timeseries for these subcatchments with the timeseries of the meteostations. To choose the meteostations for each subcatchment, we evaluated the model fit for different combinations. Using the Payerne station data for the Arbogne catchment sand the Chables station data for the Petit Glâne yielded the best model fit and lowest percentage bias. The newly aggregates timeseries of RhiresD gridded data and the two station timeseries are made available here: https://doi.org/10.5281/zenodo.17243147 (Heinz, 2025).

Replacing gridded data with station data for subcatchments Petit Glane and Arbogne (uncalibrated model):

RhiresD, default dataset

RhiresD + Payerne station data for Arbogne and and Petit Glane

RhiresD + Avenches station data for Arbogne and Chables station data for Petit Glane

RhiresD + Payerne station data for Arbogne and Chables station data for Petit Glane

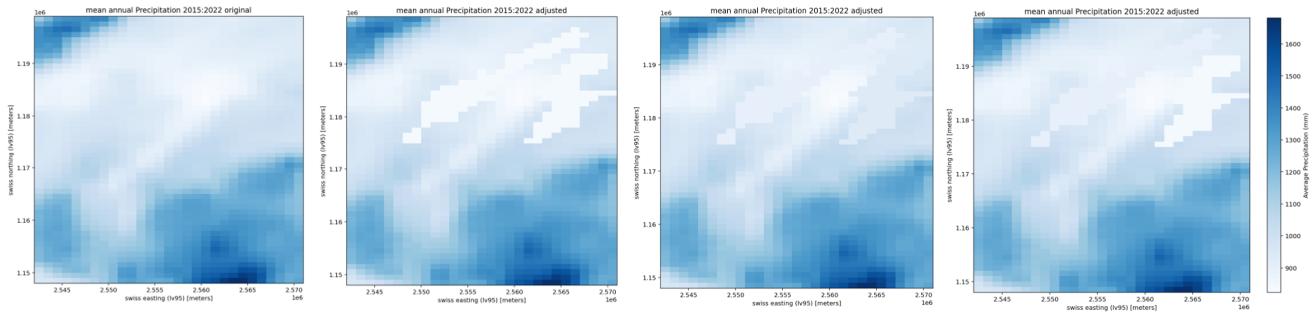

	KGE	NSE	pbias
A_A	0.62	0.51	33.4
B_P	0.58	0.64	1
F_A	0.6	0.7	5
P_G	0.64	0.65	12.8

	KGE	NSE	pbias
A_A	0.63	0.55	2.6
B_P	0.58	0.64	0.9
F_A	0.6	0.7	5
P_G	0.5	0.56	-7.2

	KGE	NSE	pbias
A_A	0.62	0.45	29.8
B_P	0.58	0.64	0.9
F_A	0.6	0.7	5
P_G	0.67	65	8.8

	KGE	NSE	pbias
A_A	0.63	0.55	2.6
B_P	0.58	0.64	0.9
F_A	0.6	0.7	5
P_G	0.67	65	8.8

A_A = Arbogne (Avenches), B_P = Broye (Payerne), F_A = Flon aval (Oron), P_G = Petit Glane (Cugy)

Figure S5. Different Combinations of the RhiresD and stationdata for the subcatchment Petit Glâne and Arbogne

S4 mHM parameters and constants

Table S2. Constants used in mHM. Column "Constant" refers to the name used in this study.

Constant	Value	Description	Name in mHM
C_{FC1}	-0.60	Constant in PTF for θ_{FC}	field_cap_c1
C_{FC2}	2.00	Constant in PTF for θ_{FC}	field_cap_c2
C_{PWPc}	1	Constant in PTF for θ_{PWP}	PWP_c
C_{PWPh}	15000	Constant in PTF for θ_{PWP}	PWP_matPot_ThetaR
C_{vG1}	1.392	Constant in PTF for n	vGenuchtenN_c1
C_{vG2}	0.418	Constant in PTF for n	vGenuchtenN_c2
C_{vG3}	-0.024	Constant in PTF for n	vGenuchtenN_c3
C_{vG4}	1.212	Constant in PTF for n	vGenuchtenN_c4
C_{vG5}	-0.704	Constant in PTF for n	vGenuchtenN_c5
C_{vG6}	-0.648	Constant in PTF for α	vGenuchtenN_c6
C_{vG7}	0.023	Constant in PTF for α	vGenuchtenN_c7
C_{vG8}	0.044	Constant in PTF for α	vGenuchtenN_c8
C_{vG9}	3.168	Constant in PTF for α	vGenuchtenN_c9
C_{Ksat1}	1.1574e-7	Constant in PTF for K_{sat}	
C_{Ksat2}	20.62	Constant in PTF for K_{sat}	
C_{Ksat3}	0.96	Constant in PTF for K_{sat}	
C_{Ksat4}	0.66	Constant in PTF for K_{sat}	
C_{Ksat5}	0.46	Constant in PTF for K_{sat}	
C_{Ksat6}	8.43	Constant in PTF for K_{sat}	

Table S3. Default and optimized mHM parameters used in this study. Column "Name (this study)" refers to the names given those parameters in the context of this study for practical reasons.

Parameter (mHM)	Unit	Default value	Calibrated value	Name (this study)
canopyInterceptionFactor	-	0.1500	0.2567	
snowTreshholdTemperature	°C	1.0000	1.4050	
degreeDayFactor_forest	$m°C^{-1}$	1.5000	3.9656	
degreeDayFactor_impervious	$m°C^{-1}$	0.5000	0.9776	
degreeDayFactor_pervious	$m°C^{-1}$	0.5000	1.9552	
increaseDegreeDayFactorByPrecip	$°C^{-1}$	0.5000	0.3843	
maxDegreeDayFactor_forest	$m°C^{-1}$	3.0000	7.8540	
maxDegreeDayFactor_impervious	$m°C^{-1}$	3.5000	7.9992	
maxDegreeDayFactor_pervious	$m°C^{-1}$	4.0000	7.9497	
orgMatterContent_forest	%	3.4000	0.0041	
orgMatterContent_impervious	%	0.1000	0.9951	
orgMatterContent_pervious	%	0.6000	0.0000	
PTF_lower66_5_constant	-	0.7600	0.7627	P_{constant}
PTF_lower66_5_clay	-	0.000900	0.000122	P_{clay}
PTF_lower66_5_Db	-	-0.2640	-0.3160	P_{BD}
PTF_higher66_5_constant	-	0.8900	1.1042	
PTF_higher66_5_clay	-	-0.0010	0.0048	
PTF_higher66_5_Db	-	-0.3240	-0.1002	
rootFractionCoefficient_forest	-	0.9700	0.9705	
rootFractionCoefficient_impervious	-	0.9300	0.9850	
rootFractionCoefficient_pervious	-	0.0200	0.9753	
infiltrationShapeFactor	-	1.7500	2.3038	$\mathrm{e}_{\mathrm{soil\_moisture}}$
rootFractionCoefficient_sand	-	0.0200	0.9753	f_{sand}
rootFractionCoefficient_clay	-	0.0200	0.9753	f_{clay}
FCmin_glob	-	0.1500	0.1500	θ_{min}
FCdelta_glob	-	0.2500	0.2500	θ_{global}
jarvis_sm_threshold_c1	-	0.5000	0.5161	T_{jarvis}
imperviousStorageCapacity	cm	0.5000	4.9946	
minCorrectionFactorPET	-	0.9300	0.8664	
maxCorrectionFactorPET	-	0.1900	0.1598	
aspectTresholdPET	-	171.00	160.22	
interflowStorageCapacityFactor	mm	85.000	82.543	
interflowRecession_slope	-	7.0000	4.0930	
fastInterflowRecession_forest	-	1.5000	1.0324	
slowInterflowRecession_Ks	-	15.0000	2.7844	
exponentSlowInterflow	-	0.1250	0.2985	
rechargeCoefficient	-	35.000	14.867	
rechargeFactor_karstic	-	-1.000	-1.000	

S5 Adjustment of bulk density representation and calculation in mHM

According to Ruehlmann and Körschens (2009) and Robinson et al. (2022), the rate of change in bulk density (ρ_b) following an increase in SOC should increase with increased initial ρ_b. This is not the case, however, in the current representation of how SOC can affect ρ_b in mHM. Currently, input to the model should be mineral ρ_b (Dbm), which is then adjusted to total ρ_b (Db):

$$\text{Db} = \frac{100}{\left(\frac{pOM}{\text{BulkDens\_OrgMatter}}\right) + \left(\frac{100 - pOM}{\text{Dbm}}\right)} \tag{S1}$$

Where pOM is a calibration parameter adjusting the percentage of organic matter in the soil (statically, over all cells), and $BulkDens\_OrgMatter$ is the ρ_b of organic matter. Since we want to be able to represent different scenarios of SOC increases, we also want this to be reflected in the ρ_b, as an increase in SOC has been observed to decrease ρ_b (Rawls et al., 2004; Chalise et al., 2019; Haruna et al., 2020). To overcome the limitation of adjusting the pOM parameter statically for all cells, we mute this part in the model and instead use already adjusted ρ_b values as input. To this end, we estimate ρ_b from initial and perturbed distributed SOC input data via the PTF by Manrique and Jones (1991), adopted by De Vos et al. (2005):

$$\rho_b = 1.660 - 0.318\sqrt{\text{SOC}} \tag{S2}$$

S6 Simulated discharge timeseries for SOC scenarios

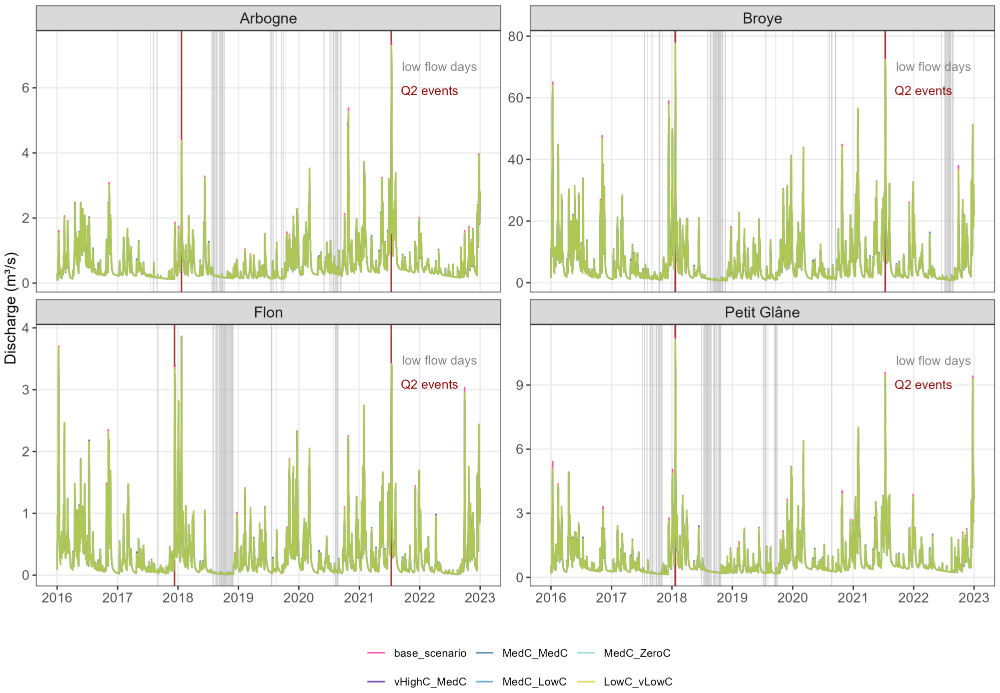

Figure S6. Discharge for all subcatchments and SOC scenarios. Gray vertical lines = days where the low flow threshold for each subcatchment is reached in the base scenario, red vertical lines = days where Q2 threshold is reached.

S7 Sensitivity in relative increase in PAWC base vs. SOC (example scenario MedC_lowC) to sand content

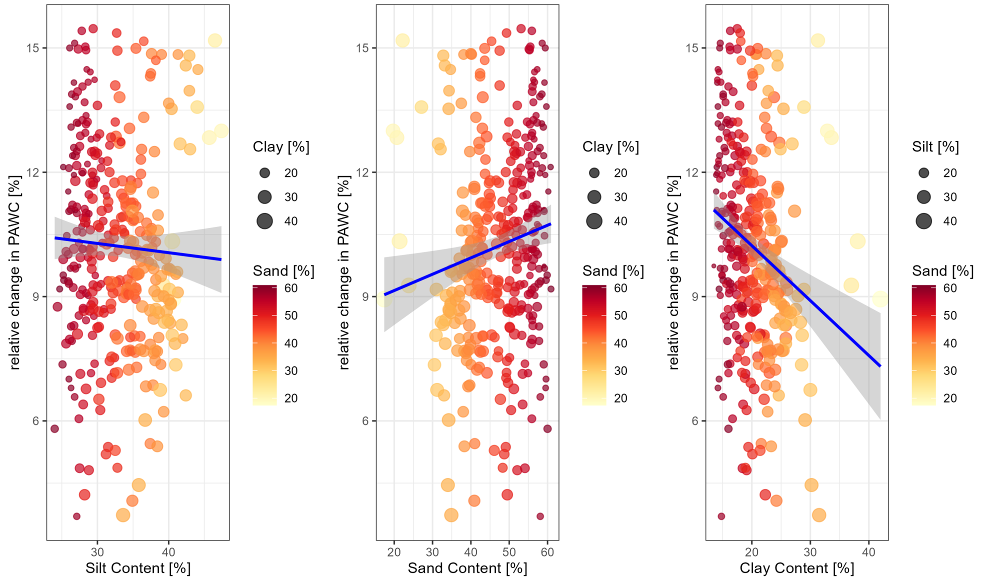

Figure S7. Relative difference in PAWC for SOC cs. base scenario for different soil textures. We can see, that PAWC increase is more sensitive to higher sand contents.

References

Brunner, M. I., Bjornsen Gurung, A., Zappa, M., Zekollari, H., Farinotti, D., and Stahli, M.: Present and future water scarcity in Switzerland: Potential for alleviation through reservoirs and lakes, Sci Total Environ, 666, 1033–1047, https://doi.org/10.1016/j.scitotenv.2019.02.169, 2019.

Chalise, K. S., Singh, S., Wegner, B. R., Kumar, S., Pérez-Gutiérrez, J. D., Osborne, S. L., Nleya, T., Guzman, J., and Rohila, J. S.: Cover Crops and Returning Residue Impact on Soil Organic Carbon, Bulk Density, Penetration Resistance, Water Retention, Infiltration, and Soybean Yield, Agronomy Journal, 111, 99–108, https://doi.org/10.2134/agronj2018.03.0213, 2019.

De Vos, B., Van Meirvenne, M., Quataert, P., Deckers, J., and Muys, B.: Predictive Quality of Pedotransfer Functions for Estimating Bulk Density of Forest Soils, Soil Science Society of America Journal, 69, 500–510, https://doi.org/10.2136/sssaj2005.0500, 2005.

Haruna, S. I., Anderson, S. H., Udawatta, R. P., Gantzer, C. J., Phillips, N. C., Cui, S., and Gao, Y.: Improving soil physical properties through the use of cover crops: A review, Agrosystems, Geosciences & Environment, 3, https://doi.org/10.1002/agg2.20105, 2020.

Heinz, M.: Precipitation input file aggregated from RhiresD and stationdata for the Broye catchment, https://doi.org/10.5281/zenodo.17243147, 2025.

Lehning, M., Völksch, I., Gustafsson, D., Nguyen, T. A., Stähli, M., and Zappa, M.: ALPINE3D: a detailed model of mountain surface processes and its application to snow hydrology, Hydrological Processes, 20, 2111–2128, https://doi.org/10.1002/hyp.6204, 2006.

Manrique, L. A. and Jones, C. A.: Bulk Density of Soils in Relation to Soil Physical and Chemical Properties, Soil Science Society of America Journal, 55, 476–481, 1991.

MeteoSwiss: Daily Precipitation (final analysis): RhiresD, https://opendatadocs.meteoswiss.ch/c-climate-data/c3-ground-based-climate-data#data-download, 2021.

MeteoSwiss: Combiprecip (CPC), https://opendatadocs.meteoswiss.ch/d-radar-data/d1-precipitation-radar-products, 2025a.

MeteoSwiss: Climate stations - Homogeneous data series, https://opendatadocs.meteoswiss.ch/c-climate-data/c1-climate-stations_homogeneous, 2025b.

MeteoSwiss, F. O. o. M. and Climatology: Daily Precipitation Ensemble: RhydchprobD, 2019.

Michel, A., Schaefli, B., Wever, N., Zekollari, H., Lehning, M., and Huwald, H.: Future water temperature of rivers in Switzerland under climate change investigated with physics-based models, Hydrology and Earth System Sciences, 26, 1063–1087, https://doi.org/10.5194/hess-26-1063-2022, 2022.

Muelchi, R., Rössler, O., Schwanbeck, J., Weingartner, R., and Martius, O.: An ensemble of daily simulated runoff data (1981–2099) under climate change conditions for 93 catchments in Switzerland (Hydro-CH2018-Runoff ensemble), Geoscience Data Journal, 9, 46–57, https://doi.org/10.1002/gdj3.117, 2021.

Rawls, W. J., Nemes, A., and Pachepsky, Y.: Effect of soil organic carbon on soil hydraulic properties, pp. 95–114, Developments in Soil Science, ISBN 9780444517050, https://doi.org/10.1016/s0166-2481(04)30006-1, 2004.

Robinson, D. A., Thomas, A., Reinsch, S., Lebron, I., Feeney, C. J., Maskell, L. C., Wood, C. M., Seaton, F. M., Emmett, B. A., and Cosby, B. J.: Analytical modelling of soil porosity and bulk density across the soil organic matter and land-use continuum, Sci Rep, 12, 7085, https://doi.org/10.1038/s41598-022-11099-7, robinson, D A Thomas, A Reinsch, S Lebron, I Feeney, C J Maskell, L C Wood, C M Seaton, F M Emmett, B A Cosby, B J eng Research Support, Non-U.S. Gov't England 2022/05/01 Sci Rep. 2022 Apr 30;12(1):7085. doi: 10.1038/s41598-022-11099-7., 2022.

Ruehlmann, J. and Körschens, M.: Calculating the Effect of Soil Organic Matter Concentration on Soil Bulk Density, Soil Science Society of America Journal, 73, 876–885, https://doi.org/10.2136/sssaj2007.0149, 2009.

Viviroli, D., Zappa, M., Gurtz, J., and Weingartner, R.: An introduction to the hydrological modelling system PREVAH and its pre- and post-processing-tools, Environmental Modelling & Software, 24, 1209–1222, https://doi.org/10.1016/j.envsoft.2009.04.001, 2009.

Zarrineh, N., Abbaspour, K., Van Griensven, A., Jeangros, B., and Holzkämper, A.: Model-Based Evaluation of Land Management Strategies with Regard to Multiple Ecosystem Services, Sustainability, 10, https://doi.org/10.3390/su10113844, 2018.